

Optimization of buffer layers for InGaAs/AlGaAs PIN optical modulators grown on GaAs substrates by molecular beam epitaxy

D. S. Katzer,^{a)} W. S. Rabinovich, K. Ikossi-Anastasiou, and G. C. Gilbreath
U.S. Naval Research Laboratory, 4555 Overlook Avenue, S.W., Washington, D.C. 20375-5347

(Received 10 October 1999; accepted 15 February 2000)

In this work we compare the effect of the buffer layer on the device quality and surface morphology of strained InGaAs/AlGaAs PIN multiple quantum well (MQW) modulators. We examine GaAs buffer layers and linearly graded InGaAs buffer layers. Our results indicate that for lower indium concentrations in the quantum wells (less than about 23%) better device performance and surface morphology are obtained by growing directly on GaAs. PIN MQWs with indium mole fractions higher than about 24% have better properties when a linearly graded buffer layer is used.
[S0734-211X(00)07003-7]

I. INTRODUCTION

GaAs/AlGaAs multiple quantum well (MQW) optical modulators grown by molecular beam epitaxy (MBE) on GaAs substrates have been under investigation for at least 17 years,¹ while modulators based on the strained InGaAs/AlGaAs materials system grown on GaAs have been studied for at least 9 years.² As shown in Fig. 1, these devices have optical absorption characteristics which vary with applied bias. MQW modulators are well known in their application to fiber optic communication systems. A new application of these structures is in free-space communications systems using modulated retroreflection of light. This application requires very large area devices with good electroabsorption, low surface roughness, low sheet resistivity, reasonably high breakdown voltage, and good optical quality.

A transmissive optical geometry is often advantageous because it simplifies the complexity of the system. This requires the use of a substrate that is transparent to the optical radiation of interest. We have investigated the use of strained InGaAs/AlGaAs vertical PIN MQW optical modulators for the 0.97–1.06 μm wavelength range where GaAs is transparent. We have recently demonstrated that these strained structures can be used in a 4 Mbps modulating retroreflector free-space communications system with a bit error rate below 10^{-6} and only 170 mW power consumption.³

A critical aspect in the growth of such strained epitaxial layers by MBE is the selection of an appropriate buffer layer between the MQW and the GaAs substrate. In particular, a buffer layer must be chosen to give the smallest surface roughness possible because surface roughness causes optical scattering and hence losses in the system. In addition, the quality of the buffer layer influences the contrast ratio of the modulator (which is a function of the ratio of the unbiased and biased absorbances). Thus it is important to have narrow absorption peaks for a high quality modulator. In this work we compare the device quality and surface morphology of strained InGaAs/AlGaAs MQW modulators grown using linearly graded InGaAs buffers to those grown directly on GaAs.

II. EXPERIMENT

A. MBE system description

The modulator samples were grown in an early model Vacuum Generators V80H MBE system which uses conventional solid sources and also has a radio-frequency (rf) plasma source for the growth of GaN and related compounds. This system has eight effusion cell ports and is pumped by a 400 l/s ion pump, a titanium sublimation pump, and a 1500 l/s cryopump mounted on a high-conductance mitred elbow. The group III effusion cells are installed with two standard double-sided Conflat spacer flanges to move them back from the shutters by 1.36 in. to improve the flux uniformity^{4,5} and to reduce shutter-induced flux transients.⁶ In addition, the gallium and indium effusion cells use a “tilted insert” crucible to direct the flux toward the center of the wafer to improve the uniformity.⁷ A conical crucible effusion cell with a cold lip is used for the aluminum source. 8-nines (99.999999% pure) gallium, zone-refined 6-nines aluminum, 7-nines indium, 7-nines-5 arsenic, 6-nines beryllium, and a section of a high-resistivity float-zone-refined silicon wafer are used as the source materials. The arsenic beam equivalent pressure (BEP) was typically 15 times the total group III BEP during the InGaAs growths. The GaAs growth rate was usually 0.5 ML/s.

The substrate heater in the MBE system is a custom-made pyrolytic graphite heating element encased in pyrolytic boron nitride. This heating element was obtained for improved heater reliability for the growth of III-nitride compounds. The indium-free mounted substrate temperature was calibrated by observing the GaAs-oxide desorption temperature with reflection high-energy electron diffraction (RHEED) and with optical pyrometry, with some additional measurements made using infrared transmission spectroscopy.^{8,9} For temperatures below 400 °C (the lower temperature limit of the pyrometer), extrapolations to room temperature were used. The heater was operated with constant current without thermocouple feedback. Although we expect that the substrate temperature may change during the initial growth of smaller band gap materials on the GaAs substrate,^{8,9} especially at low substrate temperatures, we did not intentionally

^{a)}Electronic mail: katzer@estd.nrl.navy.mil

Report Documentation Page

Form Approved
OMB No. 0704-0188

Public reporting burden for the collection of information is estimated to average 1 hour per response, including the time for reviewing instructions, searching existing data sources, gathering and maintaining the data needed, and completing and reviewing the collection of information. Send comments regarding this burden estimate or any other aspect of this collection of information, including suggestions for reducing this burden, to Washington Headquarters Services, Directorate for Information Operations and Reports, 1215 Jefferson Davis Highway, Suite 1204, Arlington VA 22202-4302. Respondents should be aware that notwithstanding any other provision of law, no person shall be subject to a penalty for failing to comply with a collection of information if it does not display a currently valid OMB control number.

1. REPORT DATE 2000		2. REPORT TYPE		3. DATES COVERED 00-00-2000 to 00-00-2000	
4. TITLE AND SUBTITLE Optimization of buffer layers for InGaAs/AlGaAs PIN optical modulators grown on GaAs substrates by molecular beam epitaxy				5a. CONTRACT NUMBER	
				5b. GRANT NUMBER	
				5c. PROGRAM ELEMENT NUMBER	
6. AUTHOR(S)				5d. PROJECT NUMBER	
				5e. TASK NUMBER	
				5f. WORK UNIT NUMBER	
7. PERFORMING ORGANIZATION NAME(S) AND ADDRESS(ES) Naval Research Laboratory, 4555 Overlook Avenue, SW, Washington, DC, 20375				8. PERFORMING ORGANIZATION REPORT NUMBER	
9. SPONSORING/MONITORING AGENCY NAME(S) AND ADDRESS(ES)				10. SPONSOR/MONITOR'S ACRONYM(S)	
				11. SPONSOR/MONITOR'S REPORT NUMBER(S)	
12. DISTRIBUTION/AVAILABILITY STATEMENT Approved for public release; distribution unlimited					
13. SUPPLEMENTARY NOTES					
14. ABSTRACT					
15. SUBJECT TERMS					
16. SECURITY CLASSIFICATION OF:			17. LIMITATION OF ABSTRACT	18. NUMBER OF PAGES 5	19a. NAME OF RESPONSIBLE PERSON
a. REPORT unclassified	b. ABSTRACT unclassified	c. THIS PAGE unclassified			

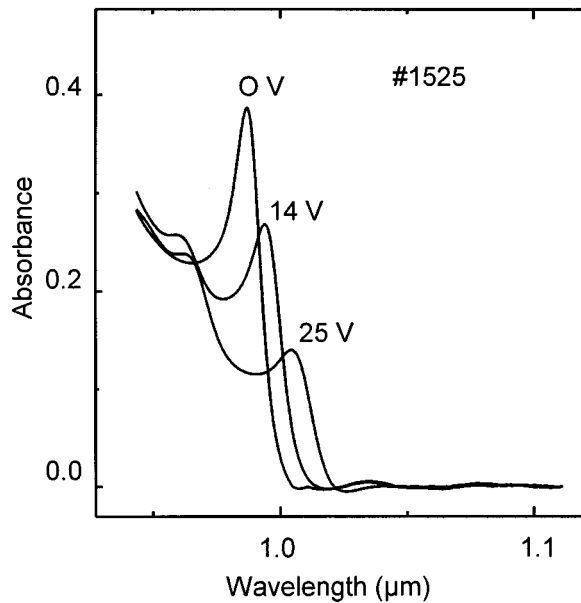


FIG. 1. Electroabsorption spectra measured on InGaAs/AlGaAs PIN multiple quantum well optical modulator No. 1525 grown on GaAs.

compensate for this effect. “MBE ready” (001) $\pm 0.5^\circ$ semi-insulating GaAs substrates were used without any additional cleaning steps. After the GaAs surface oxide was desorbed from the surface, a thin layer of GaAs was grown (typically $0.25 \mu\text{m}$) at $580\text{--}600^\circ\text{C}$ before the substrate temperature was reduced to the desired growth temperature for the PIN MQW modulator structure.

B. MBE growth parameters

The initial stages of MBE layer growth were monitored with a 10 kV RHEED system. Due to the unavoidable flux nonuniformity across the sample and the difficulty in obtaining RHEED oscillations from the geometric center of a small test sample, we did not calibrate our growth rates using RHEED intensity oscillations. We instead relied on BEP measurements made using a nude ion gauge and postgrowth measurements of test samples to calibrate our growth rates. For example, a calibration plot of \log_{10} GaAs growth rate versus \log_{10} Ga BEP is nearly linear over a fairly large range ($0.2\text{--}2.0 \text{ ML/s}$) with a correlation coefficient $R > 0.998$. We were able to obtain good run-to-run reproducibility by comparing measured BEP values with *ex situ* measurements over approximately a decade of pressure range. This calibration curve does shift over time as the source material is depleted from the crucible. As seen in Table I below, we are able to obtain excellent agreement between the designed structure and the measured structure, with the largest error being 5% in the MQW InAs mole fraction of No. 1514 (which was the first InGaAs PIN MQW MBE growth run after maintenance on the MBE system).

Growth rates were calculated by comparing optical characteristics measured at room temperature in a Fourier transform infrared (FTIR) spectrometer to those modeled by a

standard transfer matrix model which takes any strain in the layers into account.¹⁰ The GaAs/AlGaAs calibration samples for these structures was typically two 6–8 period Bragg mirror structures. The InGaAs growth rates and compositions were also extracted with this technique by growing and measuring test modulator structures. This method allows us to quickly measure our growth rates for several materials in a single sample. The excellent agreement between the measured FTIR spectrum and the modeled spectrum gives us confidence in our technique.

C. Structures examined

A series of MQWs having wells containing between 17% and 28% InGaAs was grown with and without linearly graded InGaAs buffer layers on GaAs substrates. Those structures which had linearly graded InGaAs buffer layers used a grading rate of $16\%/ \mu\text{m}$.¹¹ Table I shows the structures of the samples. Although the structures are not identical, the changes in the doping levels, the substrates, and the unstrained layer thicknesses will not appreciably change the results obtained in this study. The MQW absorption peak is primarily determined by the InAs mole fraction in the InGaAs wells and by the strain in the structure, and is only weakly affected by changes in the GaAs or AlGaAs layers. Thus we are able to make meaningful comparisons between samples even though the members of the set of samples have slightly different structures.

D. Processing steps

After MBE growth, some samples were coated with a low-temperature plasma-enhanced chemical vapor deposited (PECVD) Si_xN_y layer to act as an antireflection coating. The Si_xN_y (if present) was patterned with photoresist and removed with buffered oxide etch (BOE). A pre-evaporation clean consisting of a 30 s 1:1 BOE:H₂O etch followed by DI rinse and 30 s 1:1 HCl:H₂O etch followed by DI rinse was done prior to metal evaporation. The top surface metal was then e-beam deposited followed by a H₃PO₄:H₂O₂:H₂O mesa etch down to the conducting buffer/substrate region and a final bottom area metallization. AuGeNiAu was used for contacting the *N*-type GaAs layer, while Cr/Au was used for the *P*-type layers. The resulting devices were circular with diameters ranging from 1 to 5 mm and had both the top and bottom metals contacted from the top surface of the sample.

III. MEASUREMENTS

The finished devices were characterized in a FTIR spectrometer at room temperature. Atomic force microscopy (AFM) measurements were made in air using a Digital Instruments Dimension 3100 Nanoscope. The root-mean-square (rms) surface roughness of a $25 \mu\text{m} \times 25 \mu\text{m}$ area was calculated and is shown in Table I.

TABLE I. Structures of the InGaAs/AlGaAs PIN multiple quantum well optical modulators investigated, the measured InAs mole fraction in the wells, and the rms surface roughness measured by atomic force microscopy. The GaAs buffer layer samples are grouped together, followed by the linearly graded InGaAs buffer layer samples.

Sample	Structure	Measured InAs mole fraction in well (%)	AFM surface roughness (nm rms)
1527	3 μm $3 \times 10^{18} \text{ cm}^{-3}$ Be:GaAs 0.25 μm undoped GaAs 75 \times (28 ML 19% InGaAs/35 ML 35% AlGaAs) 0.25 μm , $3 \times 10^{18} \text{ cm}^{-3}$ Si:GaAs (001) N ⁺ GaAs substrate, 480 °C	19%	2.42
1525	1 μm $3 \times 10^{18} \text{ cm}^{-3}$ Be:GaAs 0.25 μm undoped GaAs 75 \times (28 ML 19% InGaAs/35 ML 35% AlGaAs) 500 Å undoped GaAs 0.25 μm , $3 \times 10^{18} \text{ cm}^{-3}$ Si:GaAs (001) N ⁺ GaAs substrate, 460 °C	19%	3.57
1532	0.15 μm $3 \times 10^{18} \text{ cm}^{-3}$ Si:GaAs 0.30 μm undoped GaAs 75 \times (28 ML 19% InGaAs/35 ML 35% AlGaAs) 0.25 μm undoped GaAs 1 μm , $3 \times 10^{18} \text{ cm}^{-3}$ Be:GaAs (001) SI GaAs substrate, 480 °C	22%	3.49
1514	0.2 μm $3 \times 10^{18} \text{ cm}^{-3}$ Si:GaAs 0.3 μm undoped GaAs 75 \times (28 ML 19% InGaAs/35 ML 35% AlGaAs) $3 \times 10^{18} \text{ cm}^{-3}$ 0.25 μm Be:GaAs (001) P ⁺ GaAs substrate, 480 °C	24%	4.08
1517	1 μm $3 \times 10^{18} \text{ cm}^{-3}$ Si:GaAs 500 Å undoped GaAs 50 \times (28 ML 28% InGaAs/35 ML 20% AlGaAs) 0.25 μm undoped GaAs $3 \times 10^{18} \text{ cm}^{-3}$ 0.5 μm Be:GaAs (001) P ⁻ GaAs substrate, 470 °C	28%	5.08
1424	$3 \times 10^{18} \text{ cm}^{-3}$ 0.5 μm 8% Be:InGaAs 70 \times (25 ML 17% InGaAs/28 ML 45% AlGaAs) 0.875 μm , 0%–14% graded InGaAs buffer at 16%/μm (001) N ⁺ GaAs substrate, 400 °C	17%	3.66
1526	1 μm $3 \times 10^{18} \text{ cm}^{-3}$ Be:GaAs 0.25 μm undoped 12% InGaAs 50 \times (28 ML 25% InGaAs/35 ML 20% AlGaAs) 500 Å undoped 12% InGaAs 1.125 μm , $3 \times 10^{18} \text{ cm}^{-3}$ 0%–18% graded Si:InGaAs (001) N ⁺ GaAs substrate, 450 °C	25%	9.60
1518	1 μm $3 \times 10^{18} \text{ cm}^{-3}$ Si:GaAs 500 Å undoped GaAs 50 \times (28 ML 25% InGaAs/28 ML 20% AlGaAs) 0.12 μm 12% InGaAs 1.125 μm , 0%–18% graded InGaAs at 16%/μm (001) P ⁻ GaAs substrate, 450 °C	25%	15.73

IV. RESULTS

Figure 1 shows an electroabsorption spectrum measured at room temperature for sample No. 1525, an InGaAs/AlGaAs PIN MQW modulator grown on a GaAs buffer layer. Note that the applied bias causes the peak absorption feature to shift to longer wavelengths and broaden, and the peak intensity to drop as the bias increases. These are common features of this type of modulator structure.

Figure 2 shows the zero bias absorbance measured on four InGaAs/AlGaAs PIN MQWs grown on GaAs. We can

divide the samples in the figure into two groups (1) those with peak absorbances which occur below 1.04 μm and (2) those with peak absorbances which occur at longer wavelengths. In this group of samples, the position of the absorption peak wavelength depends on the InAs mole fraction in the well. We see that sample Nos. 1527 and 1532, with 19% and 22% InGaAs in the wells, respectively, have quite similar peak absorbances and linewidths. We see the intensity of the absorption feature has decreased and its width has broadened for sample No. 1514 which has 24% InGaAs in the

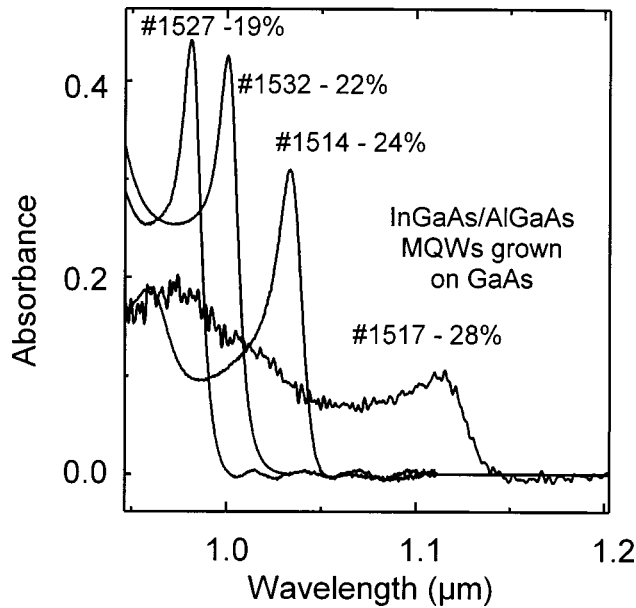


FIG. 2. Zero-bias absorption spectra of InGaAs/AlGaAs PIN multiple quantum well optical modulators grown on GaAs. The sample numbers and the indium concentrations in the wells are indicated.

wells. Sample No. 1517 has a very broad absorption feature with low intensity, indicating the sample has been severely damaged by the strain resulting from the lattice mismatch between the 28% InGaAs wells and the AlGaAs barriers (and the GaAs substrate).

Figure 3 shows the zero bias absorbance measured on four InGaAs/AlGaAs PIN multiple quantum well superlattices, two of which were grown on GaAs and two of which

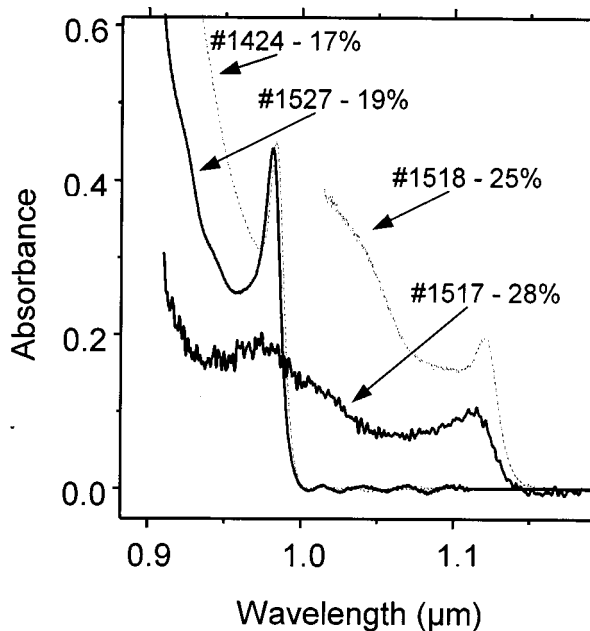


FIG. 3. Zero-bias absorption spectra of InGaAs/AlGaAs PIN multiple quantum well optical modulators grown on GaAs buffer layers (solid curves, sample Nos. 1517 and 1527) and on linearly graded InGaAs buffer layers (dotted curves, sample Nos. 1424 and 1518). The percentages list the InAs mole fraction in the wells.

were grown on linearly graded InGaAs buffer layers. Note that the absorbance peaks near 980 nm have nearly identical intensity and linewidth. These two peaks are from sample No. 1424, grown with a linearly graded InGaAs buffer layer, and sample No. 1527 which was grown with a GaAs buffer layer. The zero bias optical characteristics are similar, yet AFM measurements shown in Table I indicate that sample No. 1527 has a smoother surface. Also note that while the absorption peaks are nearly identical, the indium concentrations in the MQWs are different (17% for No. 1424, 19% for No. 1527). Since the linearly graded buffer layer introduces complexity into the growth, increases the growth time, does not improve the optical properties, and in fact degrades the surface morphology, we conclude that for PIN MQW modulators which operate near 980 nm there is no benefit to using graded InGaAs buffer layers.

On the other hand, Fig. 3 shows that there is a benefit to using graded InGaAs buffer layers for PIN modulator structures operating at longer wavelengths. We see that sample No. 1518 which was grown using a linearly graded InGaAs buffer layer has a stronger absorbance peak with a narrower linewidth than sample No. 1517 which was grown with a GaAs buffer layer. Also note that Fig. 3 shows that higher InAs mole fractions are needed to achieve the same MQW absorption peak in structures without linearly graded buffer layers because they are more relaxed than those grown on graded InGaAs buffer layers.

Figures 2 and 3 show that there is not a simple relationship between the peak absorbance wavelength and the indium concentration in the wells (see Nos. 1514, 1517, and 1518). Nos. 1514 and 1517, both grown on GaAs buffer layers, have indium concentrations which differ by 4% and different peak absorbance wavelengths while No. 1518, grown on a linearly graded InGaAs buffer layer, has a 3% lower indium mole fraction and the same peak absorbance wavelength as No. 1517. This seemingly confusing result is a reflection of the differences in strain in the structures. Strained InGaAs/AlGaAs MQW modulators with less strain relaxation in the wells will have peak absorbances at longer wavelengths than those which are more relaxed.

The AFM roughness data shown in Table I shows that the rms surface roughness increases on PIN MQW structures grown on GaAs buffer layers with increasing InAs mole fraction in the InGaAs wells, and similarly for structures grown with linearly graded InGaAs buffer layers. We also note that the samples with GaAs buffer layers have slightly smoother surfaces than those samples of similar InAs mole fractions grown with InGaAs buffer layers. The roughest sample, No. 1518, was grown with a linearly graded InGaAs buffer layer. While it shows better absorbance characteristics than No. 1517 which was grown with a GaAs buffer layer, it is substantially rougher. We believe this is due to the difficulty in precisely matching the grading of the InGaAs buffer layer (and hence its lattice constant) to MQW, and the difficulty in matching the strain in the MQW to the surface contact layer (which is InGaAs in some cases). We believe it is possible to reduce the roughness of the structures with lin-

early graded InGaAs buffer layers by more careful optimization of the structure, but this may necessitate accurate *in situ* monitoring of the InGaAs composition and growth rate. While the surface roughness is quite large in some of the samples, it is only when the surface roughness exceeds a critical value that it becomes important. Specifically, only when the surface roughness causes the optical path length to exceed 1/15 of the wavelength is it large enough to cause scattering, which puts the acceptable rms roughness limit at 26 nm. So even our roughest sample, No. 1518, is smooth enough to pass this limit. However, smoother surfaces are still desirable to improve the device yield.

The absorption data shown in Figs. 2 and 3 lead us to the following conclusions. First, the zero-bias absorption peak of our PIN MQW modulators grown on GaAs buffers does not degrade until the indium mole fraction in the quantum wells is increased beyond 22%. For these low indium concentrations, there is no apparent benefit to using linearly graded InGaAs buffer layers in these structures. For structures intended to operate beyond about 1.04 μm , which require indium mole fractions around 24% and higher, there is a clear benefit to using linearly graded InGaAs buffer layers to help reduce the strain in the structures and improve their optical absorbance characteristics. The transition region between the regions where the two buffers are preferable seems to be around 23% InGaAs.

V. CONCLUSIONS

Our results indicate that for lower indium concentrations (less than about 23%) in the MQW, better PIN MQW modulator device performance is found by growing directly on GaAs than on linearly graded InGaAs buffer layers. MQWs with indium mole fractions higher than about 24% have better properties when a linearly graded InGaAs buffer layer is

used. If an InGaAs/AlGaAs PIN MQW is grown without a linearly graded buffer layer, a higher InAs mole fraction will be needed in the wells to achieve the desired wavelength than if it were grown on a graded InGaAs buffer layer. Improvements of the device structure with linearly graded InGaAs buffer layers are possible, but tighter control of the InGaAs growth rate and composition using *in situ* monitoring may be necessary.

ACKNOWLEDGMENTS

The authors acknowledge H. B. Dietrich for his support and encouragement, and J. A. Mittereder for his help with the AFM measurements. D.S.K. also thanks J. E. Yater for careful reading of the manuscript and helpful suggestions. We thank the reviewers for their helpful comments and suggestions. This work was supported in part by the Office of Naval Research.

¹D. A. B. Miller, D. S. Chemla, D. J. Eilenberger, P. W. Smith, A. C. Gossard, and W. T. Tsang, *Appl. Phys. Lett.* **41**, 679 (1982).

²L. Buydens, P. Demeester, P. De Dobbelaere, and P. Van Daele, *Proc. SPIE* **1362**, 50 (1991).

³G. C. Gilbreath, W. S. Rabinovich, R. Mahon, M. R. Corson, M. Ferraro, D. S. Katzer, K. Ikossi-Anastasiou, T. Meehan, and J. F. Klein, *Proc. SPIE* **3807** (1999).

⁴Z. R. Wasilewski, G. C. Aers, A. J. SpringThorpe, and C. J. Miner, *J. Cryst. Growth* **111**, 70 (1991).

⁵G. C. Aers and Z. R. Wasilewski, *J. Vac. Sci. Technol. B* **10**, 815 (1992).

⁶F. G. Celii, Y. C. Kao, E. A. Beam III, W. M. Duncan, and T. S. Moise, *J. Vac. Sci. Technol. B* **11**, 1018 (1993).

⁷A. J. SpringThorpe, A. Majeed, C. J. Miner, Z. R. Wasilewski, and G. C. Aers, *J. Vac. Sci. Technol. A* **9**, 3175 (1991).

⁸B. V. Shanabrook, R. J. Waterman, J. L. Davis, R. J. Wagner, and D. S. Katzer, *J. Vac. Sci. Technol. B* **11**, 994 (1993).

⁹D. S. Katzer and B. V. Shanabrook, *J. Vac. Sci. Technol. B* **11**, 1003 (1993).

¹⁰G. Beadie, W. S. Rabinovich, D. S. Katzer, and M. Goldenberg, *Phys. Rev. B* **55**, 9731 (1996).

¹¹H. C. Chui and J. S. Harris, Jr., *J. Vac. Sci. Technol. B* **12**, 1019 (1994).